Investigating topographic neural map development of the visual system

Daniel Clark

Department of Electrical Engineering

May 10, 2013

Overview

- Most complex, efficient (and elegant?) information processor known
- How do the architecture and neural response cooperate to encode images?
- How does this network develop?
- Can we simulate and experiment with this?

Goals

- Develop intuition on visual system architecture
- Understand this in context of self-organizing map models
- Validate Topographica's core model and implementation
- Consider potential uses for and takeaways from software package

Visual System

- Retinal photoreceptors (rods, cones)
- Bipolar cells
- Retinal ganglion cells (RGC)
- Optic nerve
- Lateral geniculate nucleus (LGN)
- Optic radiation
- Primary visual cortex (V1)

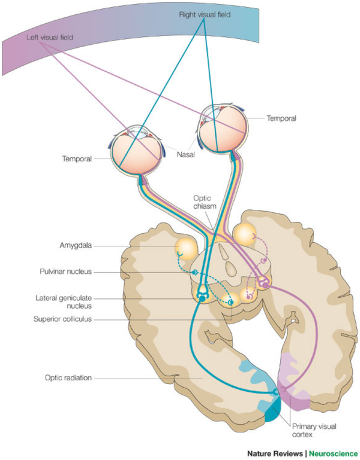

[1]

Retina

- Cones - bright environments, wavelength-sensitive (color)
- Rods - dark environments, peripheral vision
- Rods/cones synapse with bipolar cells
- Bipolar cells - ON/OFF types, temporal types, color-driven types
- Horizontal cells - feedback for photoreceptors, shape response
- Amacrine cells - tuning and control of RGC response
- RGC's - relay response to LGN

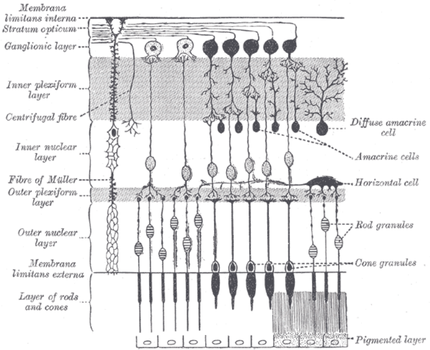

LGN

- LGN in both left and right hemisphere of brain
- Serves as relay center for many sensory systems
- A given LGN receives inputs from both eyes
- Composed of 6 layers of neural sheets
- Columnar structure of retinotopy consistent with retinal arrangement
- Credited with (some) temporal encoding
- Relays to V1 (layer 4)

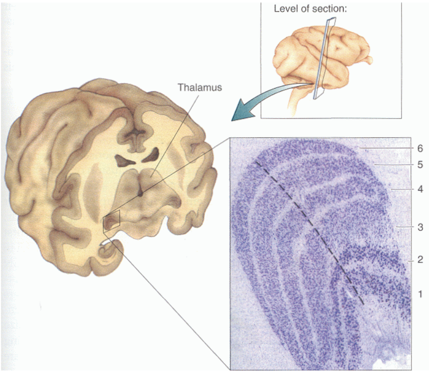

V1

- Back of left and right hemisphere of brain
- Credited with feature extraction of images
- Also composed of 6 layers of neural sheets
- Columnar structure of features (e.g. orientation)
- Complex connection architecture - afferent, lateral, feedback
- Projects to and receives feedback from higher brain centers
- Simple and complex cell types

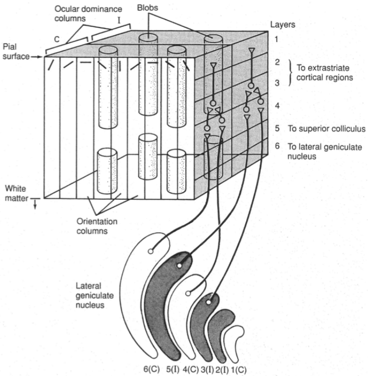

[2]

Receptive fields

- Region which defines (linear) response of neuron
- Spatiotemporal - $f(x, y, t)$
- Subcortical - difference-of-Gaussian (DoG)
- Cortical - Gabor

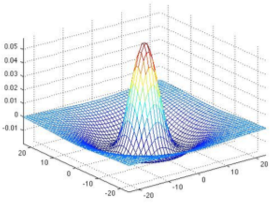

(a) DoG

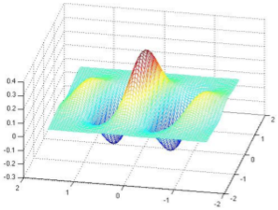

(b) Gabor

Neural responses

- Linear-nonlinear (LN) model

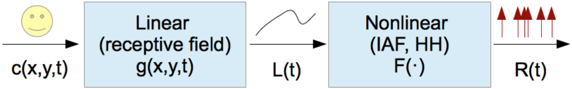

where,

$$L(t) = \int \int g(x, y, s) c(x, y, t - s) dx dy ds,$$

$$R(t) = r_0 + F(L(t)).$$

Neural responses (cont'd)

- Simple cells - phase variant, highly tuned
- Complex cells - phase invariant, broad response
- LN - great model for simple cells
- Sum together simple responses to get complex cells

$$R_{cc}(t) = R_{se}^2(t) + R_{so}^2(t) \quad [3]$$

- $R_{se}(t)$ and $R_{so}(t)$ are opposite in phase.

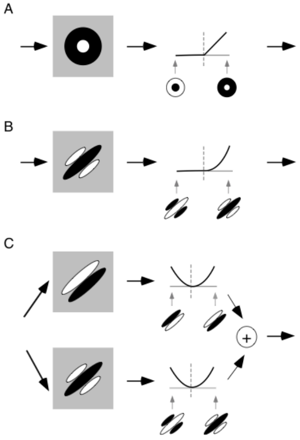

[4]

Gain control

- Natural images - large deviation in mean luminance and contrast (≈ 1000)
- Gain control - adaptability to broad range of conditions, dynamic range
- Underlying physiological mechanism?
- Mainly associated in the retina - horizontal, amacrine, bipolar cells, and LGN

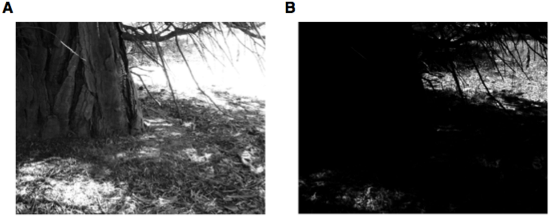

[5]

Divisive normalization and pooling

- Efficient coding theory - exploit statistical dependencies of input
- Traditionally accomplished via linear transforms (ICA)
- Non-linear - more realistic because of occlusion, simple/complex cell response [6]
- Divisive normalization (DN) - scaling of input by nonlinear function of its weighted combination

$$\mathbf{y} = \phi(\mathbf{x}) = \frac{\mathbf{x}}{f(\alpha, ||\mathbf{x}||)}$$

- Often termed "pooling" of neuron responses
- Benefits in mitigating noise, adaptability, cooperation of neurons

Self-organizing maps

- 10^{11} neurons and 10^{14} synaptic connections in brain vs. 10^{9} transistors on-chip
- Genome only contains 10^{5} genes or less
- How to get 10^{14} from 10^{5}?
- System must adapt on its own, self-organize

Plasticity

- Feature extraction requires correlations between neuronal responses and features of visual stimuli
- Correlations are not inherent from prenatal development, neurons must adapt short and long-term
- Neuron can adjust its influence over its connections, synaptic plasticity
- Input-driven development, neural maps form as a result of input statistics (Hubel and Weisel), Plato's cave
- Hebbian learning, weighting the connection strengths - "fire together, wire together"

Connectivity

- Afferent - feedforward connections, excitatory, preserves retinatopy
- Lateral - excitatory, inhibitory
- Feedback - excitatory, inhibitory
- Each neuron has a connection field

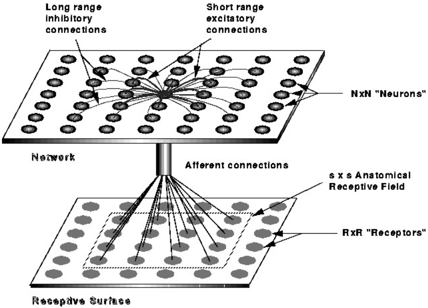

[7]

Setup

- Laterally interconnected synergetically self-organizing map
- Topographically organized neural sheet forms V1
- Each neuron in V1 has:
  - Afferent (excitatory) connections
  - Short-range lateral (excitatory) connections
  - Long-range lateral (inhibitory) connections
- Lateral connections are order of magnitude weaker than afferent, especially long-range
- Biological merit as neurons actually have these types of connections, long-range lateral have fewer synapses on postsynaptic neurons
- Point firing-rate (non-spiking) framework

Input presentation

- Input space modeled as a vector of photoreceptor activations
- Each afferent connection to V1 has non-negative associated strength (weight) which scales input
- Neuron forms an initial firing response

$$\eta_j(t_0) = f\left(\sum_{i \in h} \omega_{ij} c_i(t_0)\right) \tag{1}$$

- $\eta_j(t_0)$ - postsynaptic neuron j's initial response
- h - afferent connection field (elements of vector)
- ω_{ij} - weight from visual unit i to neuron j
- $c_i(t_0)$ - initial stimulus at unit i at time t_0
- f - nonlinear activation function

Activation function

- Nonlinear stage of LN model:

$$f(x) = \begin{cases} 0 & x \leq \delta, \\ (x-\delta)/(\beta-\delta) & \delta < x < \beta \\ 1 & x \geq \beta \end{cases}$$

- $f(x)$ - piecewise-linear sigmoid approximation
- δ - activation threshold
- β - saturation threshold

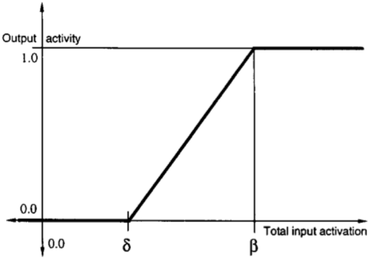

[8]

Lateral connection influence

- Lateral influence adjusts neuron response for next time step

$$\eta_j(t+dt) = f\left(\sum_{i \in h} \omega_{ij} c_i(t+dt) + \gamma_e \sum_{k \in \ell} \xi_{e,kj} \eta_k(t) - \gamma_i \sum_{k \in \ell} \xi_{i,kj} \eta_k(t)\right) \tag{2}$$

- dt - discretized time step
- γ_e - excitatory overall connection strength
- γ_i - inhibitory overall connection strength
- ℓ - lateral connection field
- $\xi_{e,jk}$ - excitatory weight from presynaptic laterally connected neuron k
- $\xi_{i,jk}$ - inhibitory weight from presynaptic laterally connected neuron k

Weight updates

- Weights are updated on a separate (longer) timescale, n, via Hebbian learning rule to allow for activity settling in network
- For afferent weights:

$$\omega_{ij}^{n+1} = \frac{\omega_{ij}^{n} + \alpha\eta_j(t_n)c_i}{\{\sum_{i\in h}[\omega_{ij}^{n} + \alpha\eta_j(t_n)c_i]^2\}^{1/2}} \qquad (3)$$

- For lateral weights:

$$\xi_{jk}^{n+1} = \frac{\xi_{jk}^{n} + \alpha_L\eta_j(t_n)\eta_k(t_n)}{\sum_{k\in\ell}[\xi_{jk}^{n} + \alpha_L\eta_j(t_n)\eta_k(t_n)]} \qquad (4)$$

- α - the Hebbian learning rate (for afferent or L lateral connections)
- t_n - time when weights are updated

Weight updates (cont'd)

- Biological plausibility for:
  - Simultaneous development of afferent and lateral connections - Has been reported in the cat [9] where afferent connections form ocular dominance columns in V1 as the lateral connections evolve to begin extracting features
  - Hebbian rule allows for normalization - Neurons conserve synaptic resources [10], this allows the model to assume total synaptic strength to be constant
  - Weight normalization over neuron as a unit - Argued in [8] that summing over all weights of a neuron converges to the same result as biologically-grounded synaptic inhibition methods found in [11] as long as numerous synapses are located locally on the neuron

Activation function updates

- Activation function updated on same timescale as weights, n

$$\delta_j^{n+1} = \min(\delta_j^n + \alpha_\delta \eta_j, \delta_{max})$$
$$\beta_j^{n+1} = \max(\beta_j^n + \alpha_\beta \eta_j, \beta_{min}).$$

- α_δ - update learning rate for response threshold
- α_β - update learning rate for saturation threshold
- Provides for additional nonlinearity in neural response - as $f(x)$ becomes narrower, firing rate will vary more easily
- Biological plausibility - immature neurons fire more easily, linearly. Mature neurons harder to depolarize, but because of developed ion channels at synapse it fires stronger [12]

Connection death

- “Prune” weak lateral connections after time duration

$$
\begin{aligned}
\text{if } \xi_{kj} &< w_c \text{ after initial time } t_o, \\
\text{then } \xi_{kj} &= 0; \\
\text{else if } \xi_{kj} &< w_c \text{ after subsequent intervals } t_c \\
\text{then } \xi_{kj} &= 0
\end{aligned}
$$

- Model gives the connection weights a timeframe to recover before death as opposed to immediate removal
- Biological plausibility - has been observed in many cases where the majority of long-range lateral connections don't survive cortical development [9]

LISSOM methodology review

1. Afferent weight vectors initially randomly distributed, lateral weight vectors randomly distributed at various radii d for excitatory, and d' for inhibitory; total weight of each set is fixed to 1.0
2. Image presentation - initial neuron response proportional to similarity of input and afferent weights
3. Response refined through lateral interaction
4. Activity settles over multiple time steps, dt, to form activity “bubbles”
5. Time step hits t_n when the weight and activation updates take place
6. New image presentation, and repeat
7. Lateral connections are pruned at t_o and subsequent t_c intervals

LISSOM performance

- Initially random input afferent weights
- Each weight vector is transformed into the two-dimensional coordinate system and plotted as a point connected to its four immediate neighbors
- As inputs are randomly drawn, the network evolves to form a retinatopic map represented by the afferent weights (after 30,000 iterations)

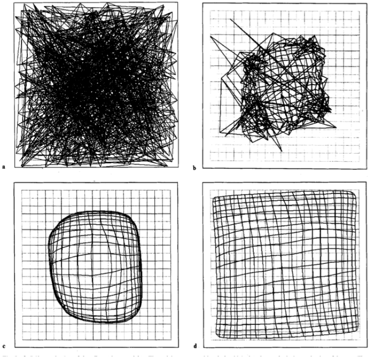

[8]

RF-LISSOM performance

- Same as LISSOM but with local, retinotopically-centered receptive fields predefined
- Ocular dominance results use two photoreceptor sheets (left and right eyes)
- Realistic results with left, right, and binocular preference

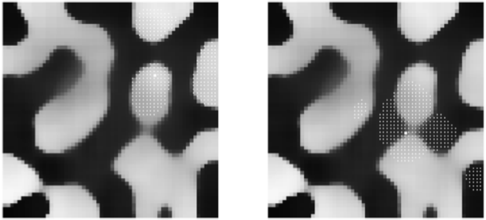

(a) Connections of a Monocular Neuron (a) Connections of a Binocular Neuron [13]

LISSOM takeaways

- Great base framework for map development, but certain elements lack biological plausability
- Supervised logical compare for threshold update is unrealistic
- No gain control, contrast and luminance of input could drastically affect performance

GCAL

- Gain control, adaptation, laterally connected model improves upon LISSOM
- Incorporates feedforward gain control
- Single-neuron homeostatic adaptation of firing-rate threshold
- Comprised of (at least):
  - Photoreceptor sheet
  - RGC/LGN On sheet
  - RGC/LGN Off sheet
  - V1

Initial mechanisms

- Connection field for afferent projection from photoreceptors to RGC/LGN predefined as local to neuron
- Weights are fixed as a DoG, where they take the form

$$\omega_{ij} = \alpha \exp\left(-\frac{(x_i - x_j)^2 + (y_i - y_j)^2}{2\sigma_c^2}\right) + \beta \exp\left(-\frac{(x_i - x_j)^2 + (y_i - y_j)^2}{2\sigma_s^2}\right) \tag{5}$$

- α, *beta* - positive or negative scaling factors depending on on-center or off-center
- x_i, y_i - location of presynaptic unit i in photoreceptor sheet
- x_j, y_j - location of postsynaptic neuron j in RGC/LGN sheet
- σ_c, σ_s - width of center and surround Gaussians, respectively

RGC/LGN neuron activation

- Activations are updated similar to LISSOM Eq. (1)

$$\eta_j(t + dt) = f\left(\gamma_L \sum_{i \in F_j} \omega_{ij} c_i(t)\right), \tag{6}$$

- γ_L - constant strength of afferent connections
- f - half-wave rectifier (no predefined limits)
- F_j - neuron j's DoG connection field
- ...gain control?

RGC/LGN gain control

- Gain control is implemented by divisive normalization from lateral neuron's through connection weights, $\omega_{ij,S}$

$$\omega_{ij,S} = \exp\left(-\frac{(x_i - x_j)^2 + (y_i - y_j)^2}{2\sigma_S^2}\right), \tag{7}$$

- σ_S - width of Gaussian
- Gain control update of activity, on n timescale

$$\eta_j^{n+1}(t_n) = f\left(\frac{\eta_j^n(t_n)}{\gamma_S \sum_{i \in L_j} \omega_{ij,S}\eta_i^n(t_n)}\right), \tag{8}$$

- γ_S - strength scaling factor
- L_S - lateral connection field
- Gain control provides presynaptic stability of response variation

V1 activity update

- Implemented in much the same way as LISSOM, can be described more succinctly as

$$\eta_j(t+dt) = f\Big(\sum_p \gamma_p \underbrace{\big(\sum_{i \in F_{jp}} \omega_{ij,p}\eta_i(t)\big)}_{X_{jp}(t+dt)}\Big), \tag{9}$$

- p - afferent, lateral exc., or lateral inh. projection
- γ_p - strength factor for projection p, (+) for excitatory, (-) for inhibitory
- X_{jp} - contribution from projection p to neuron j
- η_j is updated throughout the presentation of a single image over multiple time steps until t_n as in LISSOM - settling process
- V1 activity is reset to 0 before the next presentation - allows for discontinuous image presentations and non-biased feature maps

V1 homeostatic activation update

- Activation function is updated as a result of average activity for each neuron
- Smoothed exponential average of neuron activity is calculated

$$\bar{\eta}_j^{n+1} = (1 - \beta)\eta_j(t_n) + \beta\bar{\eta}_j^n, \tag{10}$$

- $\beta \approx 0.999$ - smoothing parameter
- Average $\bar{\eta}_j^{n+1}$ is used to update the threshold activity for neuron j for the next presentation

$$\delta_j^{n+1} = \delta_j^n + \lambda(\bar{\eta}_j^{n+1} - \mu), \tag{11}$$

- $\lambda \approx 0.0001$ - learning rate
- μ - target activity rate (spontaneous firing)
- Provides postsynaptic stability of neuron response

V1 weights update

- Weights initialized similarly as in RGC/LGN but with cut-off radius r_p for projection p

$$\omega_{ij,p} = \begin{cases} u \exp\left(- \frac{(x_i - x_j)^2 + (y_i - y_j)^2}{2\sigma_p^2} \right), & (x_i - x_j) \leq r_p, \\ 0, & otherwise \end{cases}$$

- $u = 1$ for lateral excitatory, random scalar otherwise
- Finally, weights are updated and normalized in the same way as in LISSOM

$$\omega_{ij,p}^{n+1} = \frac{\omega_{ij,p}^{n} + \alpha \eta_j(t_n) \eta_i(t_n)}{\sum_k \left(\omega_{kj,p}^{n} + \alpha \eta_j(t_n) \eta_k(t_n) \right)}$$

GCAL performance example

- Leads to robust and stable map development - consistently developing orientation preferences throughout training and contrast invariant tuning

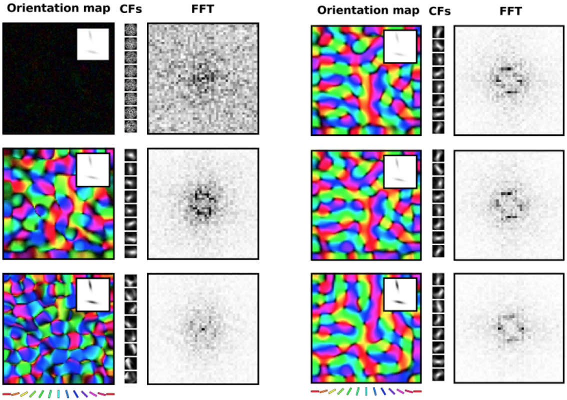

[14]

GCAL takeaways

- Biological plausibility is same or better than LISSOM
- Gain control mechanism plausible with horizontal and amacrine cells contribution
- Homeostatic adaptation converges towards spontaneous firing rate, realistic assumption
- RGC/LGN weights are most likely not fixed in vivo
- Important to keep in mind - model and results are judged on comparing simulated maps with real ones, if they match the model is a good fit

GCAL vs LISSOM

LISSOM:

- Biological Plausibile
- No aspect of gain control
- Logical compare enforced in activation function
- Model allows for continuous inputs
- Each neuron interprets entire input space

GCAL:

- Biologically plausible
- Feedforward gain control in RGC/LGN
- Activation function based on moving average
- Model assumes discontinuous inputs, reset activity
- Each neuron has fixed radius connection fields

Overview

- Open source software package designed for topographic neural map development on large-scale
- Is ideal for implementing LISSOM and GCAL models
- Can interface with other languages for allocating computing tasks - C/C++, MATLAB, Python
- Also interface with small-scale, individual neuron analysis packages - GENESIS, NEST, NEURON

Setting up a network

- Architecture setup before training or testing, user-specified
- Minimally must have a photoreceptor sheet and cortical sheet, but more are common
- User must also specify connection field types between sheets and how they project to postsynaptic units
- A wide range of built-in visual patterns and user image files can be presented

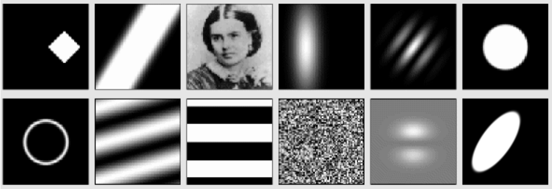

[15]

Basic features

- Calculation of weights, presynaptic, postsynaptic activity is completely customizable
- Once network is setup, can be ran over *n* iterations, or stepped through by *dt* timescale
- Throughout the training process, one can view network results including sheet activity, individual connection strengths, sheet-wide projections
- Feature preference can also be viewed (e.g. orientation), however, these calculations can take a while

Interfacing

- Topographica can use outside simulators to compute the response of input activity, including spiking neuron models (NEST, NEURON)
- Accomplished by exporting activity through a Python wrapper (e.g. PyNN), specifying run time and number of neurons
- Import matrix of spike times for each neuron from external simulator, compute average firing rate
- Use this as the activity input for the next neural sheet
- An example of this is well documented in [16]

Framework

- Each sheet represented as a two-dimensional array of neurons
- Neurons specified in sheet coordinates and matrix coordinates
- Density parameters specifies how many units are present in a 1.0 length of sheet
- Sheet size increases from cortex down to photoreceptors (1.0×1.0 to $\approx 2.75 \times 2.75$) to avoid boundary effects
- Weights are defined within connection field radius

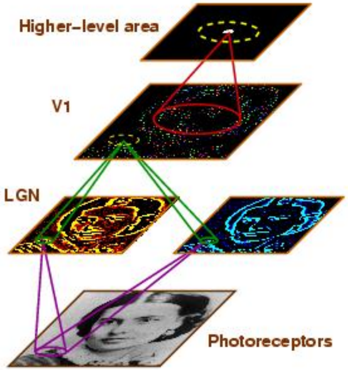

[15]

Function and sheet types

- Pattern generators, transfer, response, learning functions
- Generator sheets, projection sheets, joint normalizing continuous sheets

Input-driven development

- Patterns presented to network are crucial for how it develops
- Natural images are the best for simulating real experience
- However, for specific feature extraction, mathematical function patterns provide interesting insight
- For example, take a Gabor, human face, and line all randomly rotated and translated between presentations



Input-driven development (cont'd)

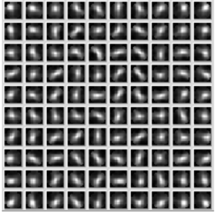

(a) Gabor trained

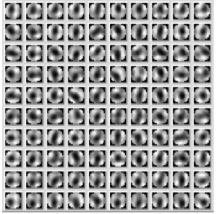

(b) Human face trained

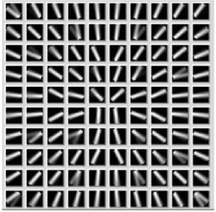

(c) Straight line trained

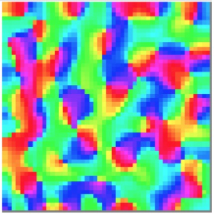

(a) Gabor trained

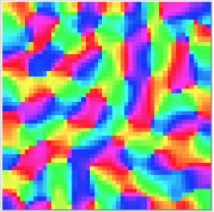

(b) Human face trained

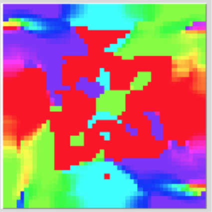

(c) Straight line trained

Complex cell development

- In [14], Topographica was utilized to show realistic development of complex cells
- Use two layers of V1, layer $4C\beta$ and layer $2/3$, only $4C\beta$ receives LGN connection directly
- Lateral connections in layer $4C\beta$ are several times weaker than in $2/3$
- Afferent projection from $4C\beta$ to $2/3$, feedback from $2/3$ to $4C\beta$
- Interesting dynamic - weak connections and random initialization cause local phase variations in $4C\beta$
- Layer $2/3$ pools together phase variance to produce complex cell-like responses
- Feedback from $2/3$ (strong lateral connections) to $4C\beta$ preservers orientation preference while traversing layers (consistent with early visual system architecture)

Complex cell development (cont'd)

- Training sequence for this model was very elaborate
- Two stages of training - prenatal (retinal waves), post natal (natural images)
- Retinal waves simulated as a concentric ring convolved with white noise, natural images from database in [17]

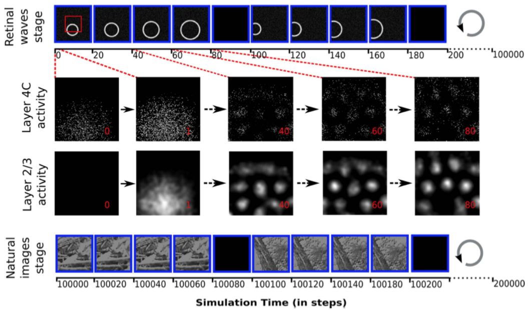

Complex cell development (cont'd)

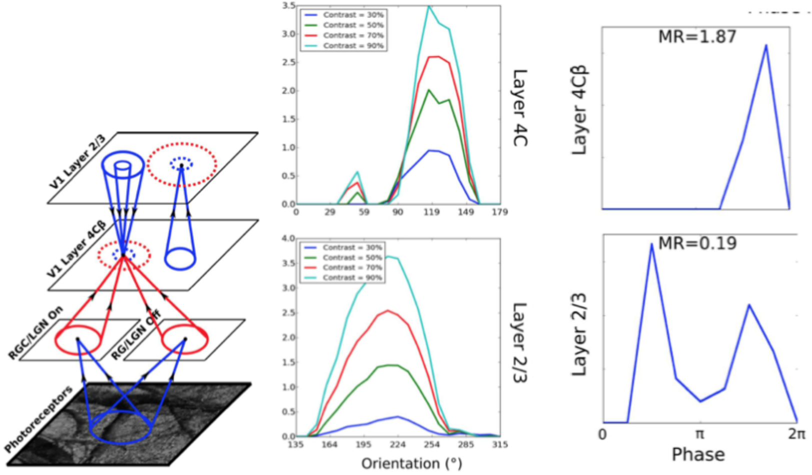

(a) Model architecture (b) Orientation contrast tuning (c) Phase tuning

[18]

TCAL

- Initial experiments were developed to derive a spatiotemporal RF by exposing a trained network to white noise and using reverse correlation

$$D(x, y, \tau) = \frac{Q_{Lc}(x, y, -\tau)}{\sigma_c^2} = \frac{1}{T}\int_0^T L(t)c(x, y, t+\tau)dt \qquad (12)$$

- $D(x, y, \tau)$ - spatiotemporal RF, $Q_{Lc}(x, y, \tau)$ - correlation of white noise stimulus and output firing rate $L(t)$ of neuron
- However, the built-in models were all setup to reset V1 activity between input presentations
- Develops of Topographica are working on TCAL (Temporally CALibrated GCAL) to integrate with training to test on continuous inputs [19]

Further research

- Find relationship between afferent projection weights and receptive field of cortical unit to give a quantitative measure of the impact of lateral connectivity
- Evaluate encoding performance of different stimuli on various models, and training input patterns
- Integration of spiking neurons for performance comparison between point firing rate units and more realistic neural behavior
- Reproduce the experimental results from early-stage models to the latest ones to develop an intuition on how each additional component influences performance
- Suggestions...?

Thanks

Special thanks to Yiyin Zhou and Nikul Ukani for directing my progress and giving feedback and suggestions on a daily basis. Thanks to Prof. Lazar for supervising the project. And thanks to the rest of the Bionet lab for various tips and consulting when I had questions.

References I

- Deborah E. Hannula, Daniel J. Simmons, and Neal J. Cohen.
  Imaging implicit perception: promise and pitfalls.
  Nature Reviews Neuroscience, 6:247–255, March 2005.

- Risto Miikkulainen, James A. Bednar, Yoonsuck Choe, and Joseph Sirosh.
  Computational Maps in the Visual Cortex.
  Springer Science+Business Media, Inc., 2005.

- Fabrizio Gabbiani and Steven James Cox.
  Mathematics for Neuroscientists.
  Academic Press, first edition, August 2010.

References II

Matteo Carandini, Jonathan B. Demb, Valerio Mante, David J. Tolhurst, Yang Dan, Bruno A. Olshausen, Jack L. Gallant, and Nicole C. Rust.
Do we know what the early visual system does?
The Journal of Neuroscience, 25(46):10577–10597, November 2005.

Fred Rieke and Michael E. Rudd.
The challenges natural images pose for visual adaptation.
Neuron, 64(5):605–616, December 2009.

Odelia Schwartz and Eero P. Simoncelli.
Natural signal statistics and sensory gain control.
Nature neuroscience, 4(8):819–825, August 2001.

References III

Joseph Sirosh, Risto Miikkulainen, and James A. Bednar.
Self-organization of orientation maps, lateral connections, and dynamic receptive fields in primary visual cortex.

Joseph Sirosh and Risto Miikkulainen.
Cooperative self-organization of afferent and lateral connections in cortical maps.
Biological Cybernetics, 71:65–78, 1994.

Edward M. Callaway and Lawrence C. Katz.
Emergence and refinement of clustered horizontal connections in cat striate cortex.
The Journal of Neuroscience, 10(4):1134–1153, April 1990.

References IV

Jean-Pierre Bourgeois, Pawel J. Jastreboff, and Pasko Rakic.
Synaptogenesis in visual cortex of normal and preterm monkeys: Evidence for instrinsic regulation of synaptic overproduction.
Proceedings of the National Academy of Sciences, 86(11):4297–4301, June 1989.

Tuevo Kohonen.
Physiological interpretation of the self-organizing map algorithm.
Neural Networks, 6:895–905, 1993.

D.A Prince and J. Huguengard.
Functional properties of neocortical neurons.
In *Neurobiology of Neocortex*, Dahlem Conference Reports, pages 153–176, New York, 1988. John Wiley and Sons.

References V

Joseph Sirosh and Risto Miikkulainen.
Topographica receptive fields and patterned lateral interaction in a self-organizing model of the primary visual cortex.
Technical Report AI94-225, The University of Texas at Austin, Austin, TX, December 1994.

Judith S. Law, Jan Antolik, and James A. Bednar.
Mechanisms for stable and robust development of orientation maps and receptive fields.
Technical Report EDI-INF-RR-1404, Institute for Adaptive and Neural Computation, University of Edinburgh, Edinburgh, Scotland, UK, 2011.

May 2013.

References VI

James A. Bednar.
Topographica: building and analyzing map-level simulations from python, c/c++, matlab, nest, or neuron components.
Frontiers in Neuroinformatics, 3(8):1–9, March 2009.

Christoph Kayser, Wolfgang Einhauser, and Peter Konig.
Temporal correlations of orientations in natural scenes.
Neurocomputing, 52-54:117–123, 2003.

Jan Antolik and James A. Bednar.
Development of maps of simple and complex cells in the primary visual cortex.
Frontiers in Computational Neuroscience, 5(17):1–19, April 2011.

References VII

Jean-Luc Richard Stevens.
A temporal model of neural acticity and vsd response in the primary visual cortex.
Master's thesis, University of Edinburgh, 2011.